ELSEVIER

Marine and Petroleum Geology 18 (2001) 525–534

Marine and Petroleum Geology

www.elsevier.com/locate/marpetgeo

Growth faults at the prodelta to delta-front transition, Cretaceous Ferron sandstone, Utah

Janok P. Bhattacharya[a,*], Russell K. Davies[b]

[a]University of Texas at Dallas, Geosciences Department, P.O. Box, 830688, Richardson, TX 75083-0688, USA
[b]Rock Deformation Research, USA Inc., P.O. Box 2998, McKinney, TX 75070-8998, USA

Received 28 December 2000; received in revised form 1 March 2001; accepted 10 March 2001

Abstract

Cliff exposures of synsedimentary growth faults at the base of the Cretaceous Ferron sandstone in central Utah represent outcrop analogs to subsurface growth faults. Delta front sands prograded over and deformed less dense prodelta muds of the underlying Tununk Shale. Detailed fault patterns and associated facies changes demonstrate a complex fault history and style for growth fault development rather than a simple progressive development of faults in a basinward position. The most proximal and most distal fault sets were the earliest active faults. Growth faulting was initiated by deposition of cross-bedded distributary channel and mouth bar sandstones that reach 9 m thick in the hangingwalls of the faults. Curvature of the beds in the hangingwall of the faults nucleates smaller conjugate fault sets. Cross-bed sets in the hangingwalls of faults decrease from meter to decimeter scale away from the faults suggesting decreasing flow velocity or decreased preservation of cross sets as a result of decreasing accommodation in distal hangingwalls. Shifts in depositional loci, including upstream and downstream accretion of mouth bar sands contribute to the complex faults history and internal heterogeneity and development of potentially isolated sandy reservoir compartments.

Keywords: Ferron sandstone; Delta; Growth fault; Listric; Normal fault

1. Introduction

Synsedimentary normal faults, or growth faults, associated with deltas are involved in the formation of major traps for oil and gas reservoirs and they may isolate compartments in subsurface hydrocarbon reservoirs or aquifers. From an environmental perspective, many coastal cities are built over areas that are affected by synsedimentary growth faulting, such as Houston, Texas.

The anatomy of natural growth fault systems is largely derived from subsurface seismic and widely-spaced well log or core data (Bishop, Buchanan, & Bishop, 1995; Busch, 1975; Diegel, Karlo, Schuster, Shoup, & Tauvers, 1995; Galloway, Hobday, & Magara, 1982). Seismic data sets can be useful for mapping and describing the regional-scale geologic architecture of growth faults, but finer-scaled details are typically not well imaged. Well log and core data invariably alias smaller scale structures. Outcrops can provide complete information about the lateral variability at a range of scales. However, previous outcrop studies of growth faulted strata do not integrate detailed sedimentological measured sections with fault kinematics and section restorations (Brown, Cleaves, & Erxleben, 1973; Edwards, 1976; Elliot & Lapido, 1981; Rider, 1978). There is thus a distinct gap in our knowledge of the interplay between fault nucleation and deposition of growth faulted strata.

In this paper, we attempt to fill this gap by integrating detailed sedimentological and stratigraphic analysis with kinematic restoration of a superbly exposed outcrop example of small-scale growth faults associated with the Cretaceous Ferron delta complex in cliffs above Muddy Creek, Utah (Fig. 1).

We address several questions:

1. Are the growth faults initiated by a specific facies or depositional process?
2. Do faults initiate in a more landward position with subsequent fault nucleation occurring in more seaward positions as the delta progrades, or do faults initiate in a more seaward position and migrate landward as a retrogressive kinematic wave?
3. Are faults reactivated?
4. How is the growth faulting accommodated?
5. What kind of sedimentologic and facies variations is associated with different positions in individual growth faults?

* Corresponding author. Tel.: +1-972-883-2401; fax: +1-972-883-2537.

0264-8172/01/$ - see front matter
PII: S0264-8172(01)00015-0

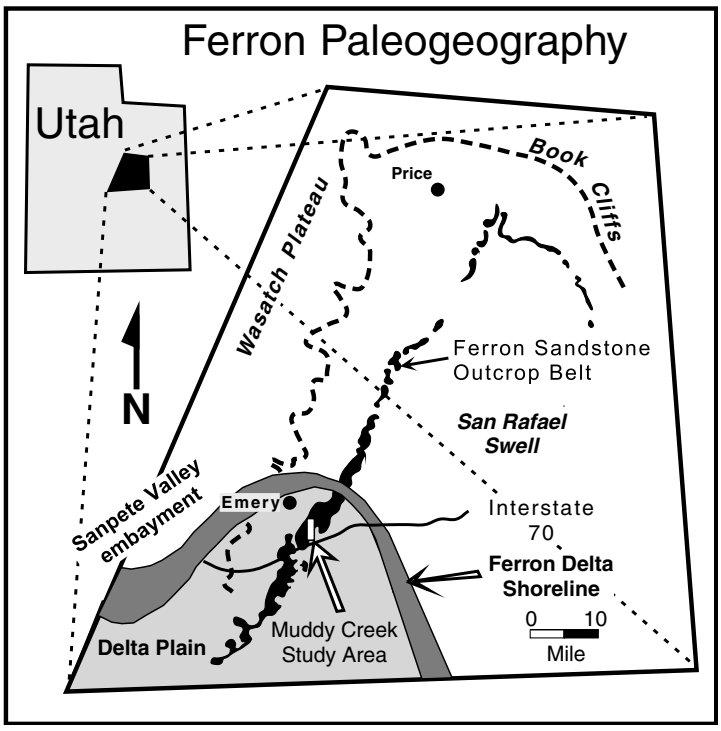

Fig. 1. Location map of study area showing the general northeast progradation of the Ferron delta. In the Muddy Creek study area the delta lobe prograded locally to the northwest into the Sanpete Valley Embayment (from Ryer & McPhillips, 1983).

2. Geology of study area

The Ferron sandstone is a fluvio-deltaic clastic wedge deposited into a rapidly and asymmetrically subsiding foreland basin that rimmed the western margin of the late Cretaceous (Turonian) seaway in central Utah (Gardner, 1995). The Ferron consists of seven regressive-transgressive stratigraphic cycles, each bounded by a flooding surface and associated coals (Gardner, 1995; Ryer, 1984). In outcrop these form a series of well-exposed sandstone cliffs separated by slope-forming mudstones. Regionally, the Ferron forms a large lobate body that prograded northwest, north, and northeast forming a large western embayment (the Sanpete Valley Embayment in Fig. 1) of the Cretaceous seaway (Ryer & McPhillips, 1983). This bay experienced diminished wave activity compared to the rest of the Cretaceous seaway and was infilled with river-dominated delta lobes.

This study focuses on a top-truncated, river-dominated delta lobe that locally prograded to the northwest into the embayment and is interpreted to be associated with a minor drop of sea level within 'short-term stratigraphic cycle 1' at the base of the 'Ferronensis Sequence' of Gardner (1995). This sea-level drop forced the deposition of delta front and prodelta mudstones onto highly bioturbated older 'shelf' mudstones of the underlying Tununk shale member of the Mancos Shale. Listric normal faults sole into this shale and growth of the section across the faults seems to occur exclusively within the delta front sands. In terms of paleogeographic reference, with respect to our outcrop, we use the term landward (or proximal) to refer to features to the southeast and seaward (or distal) to refer to features that lie to the northwest and which prograde into the Sanpete Valley Embayment (Figs. 1 and 2).

3. Data and methods

For this study we mapped three fault blocks, here referred to as proximal, intermediate and distal, that are the most landward portion of a larger fault set, exposed along the south side of Muddy Creek Valley (Fig. 2). The cliff orientation parallels paleocurrents and fault dip indicating a depositional and structural dip cross section. The larger set of faults have been studied and interpreted by Nix (1999); Morris and Nix (2000) who suggested that the faulting was accommodated by movement of mobile prodelta muds associated with shale diapirism. Our work is a more detailed analysis of the fault geometry and kinematics and associated sedimentary facies changes and distribution.

We measured 10 sedimentological sections and interpreted a photomosaic covering a lateral distance of approximately 130 m (Fig. 2). Distinctive facies geometry allowed us to determine the pre-growth, growth, and post-growth stratigraphy. Integrating facies and structure, we documented offset of specific beds across the faults. These distinctive beds are characterized by specific stacking order,

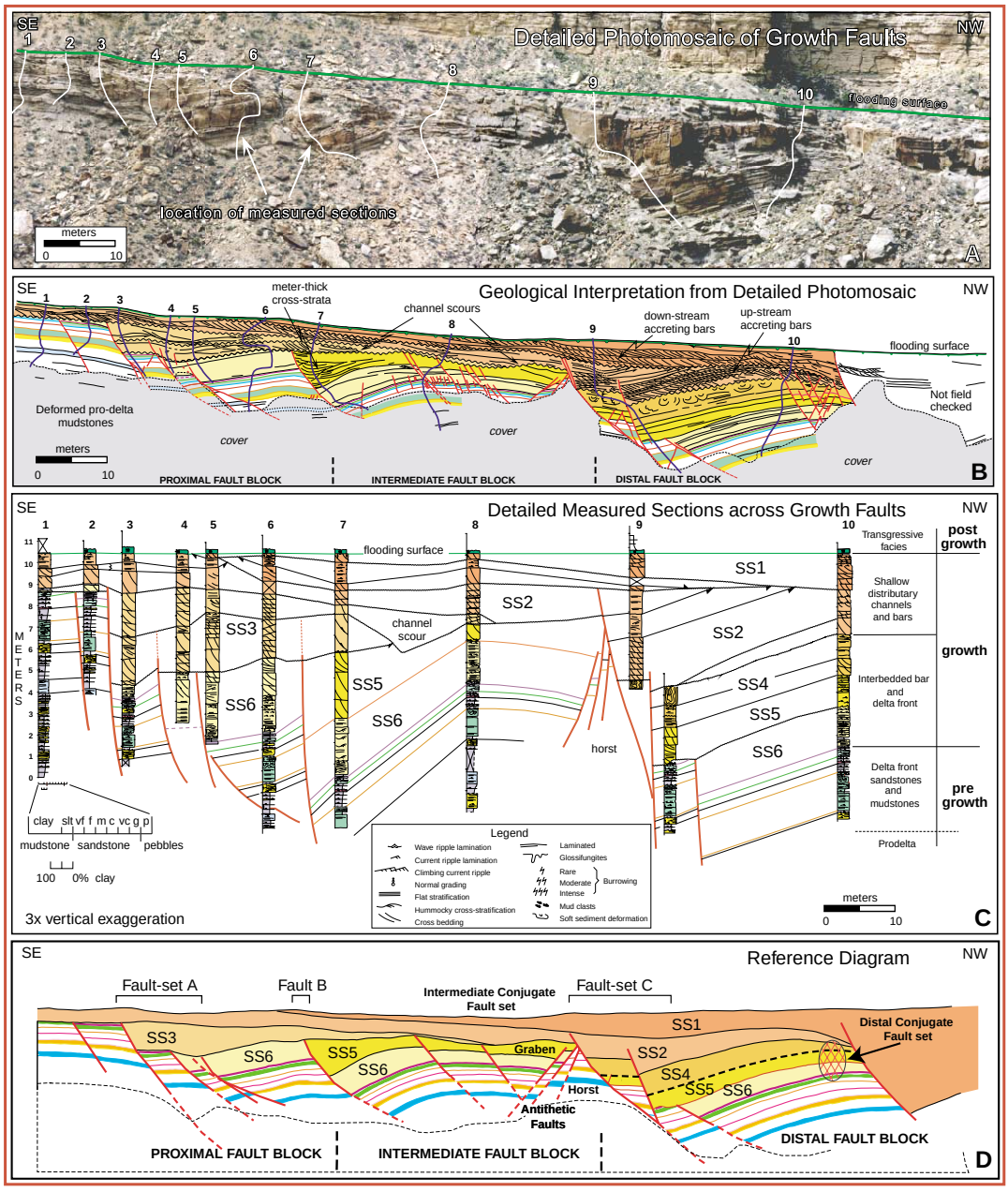

Fig. 2. Cross section of Ferron growth faults in south cliff-face of Muddy Creek showing: (A) detailed photomosaic; (B) geological interpretation of structure; (C) detailed measured sections; and (D) reference diagram. Coloured beds in the geological interpretation are matched to the sands in the measured section and show offset on faults. The growth interval consists of upstream and downstream accreting cross-bedded sandstones deposited in shallow distributary channels and proximal distributary mouth bars. The relative ages of these sands are indicated with numbers SS6–SS1 from oldest to youngest, respectively.

grain sizes, and sedimentary structures, and are designated with different colors in the measured sections (Fig. 2(C)) and structural interpretation (Fig. 2(B)). For example, at 6 m in section 1 (Fig. 2) there is a distinctive bed, about 0.5 m thick, that consists of current-rippled sandstone. This is overlain (at 7 m in Fig. 2) by another pair of sandstone beds (coloured green). The lower bed comprises about 1 m of horizontally-laminated sandstone and is overlain by about 0.5 m of deformed sandstone. This distinct triplet of beds, along with others, could be identified and correlated throughout the entire outcrop face, as illustrated in Fig. 2. The correlations and interpretations were used as the basis to constrain kinematic models for restoration of each major fault.

4. Stratigraphy and depositional facies

The outcrop interval studied forms a distinctive cliff at the base of the Ferron sandstone along Muddy Creek. It shows an overall upward-coarsening facies succession indicating progradation. Description of the pre-, growth-, and

post-growth sections below will demonstrate that these facies successions are typical of those produced by a river-dominated prograding delta front (Bhattacharya & Walker, 1992).

4.1. Pregrowth section

Basal pre-growth strata are shown as green, red and yellow sandstones interbedded with gray shales in Fig. 2. Sandstone beds are predominantly fine grained, mostly horizontally-stratified to climbing current-rippled and alternate with laminated mudstones containing abundant small-scale soft-sediment deformation features, with abundant load casts. Burrows are rare but *Planolites, Skolithos* and *Arenicolites* occur throughout the succession with rarer small diameter (<0.5 cm) *Thallasinoides*, *Ophiomorpha* and *Rosselia* observed locally.The low diversity, abundance, and small diameter of trace fossils suggests a stressed and probably brackish-water environment that is likely proximal to a river mouth (Bhattacharya & Walker, 1992; Gingras, MacEachern, & Pemberton, 1998; Moslow & Pemberton, 1988). Coalified plant debris is common on parting planes and rare larger woody clasts are bored by marine *Teredolites*. The climbing ripples, lack of burrowing, and abundant load casts and soft sediment deformation suggest high sedimentation rates and are typical of deposition in a river-dominated prodelta environment (Bhattacharya & Walker, 1992; Gingras et al., 1998; Moslow & Pemberton, 1988).

The loading indicates that the prodelta muds were less dense than overlying more-dense sandstones. Density differences result from the fact that rapidly-deposited muds typically have much higher porosity than sands (Rider, 1978).

Underlying facies are covered by rubble within the mapped outcrop, but are well exposed along the cliffs about 300 m to the south. There, the section consists of about 30 m of laminated silty mudstones with rare, very-fine grained sandstone beds and ironstone nodules. This passes up into about 7 m of deformed interbedded mudstones and sandstones showing interstratal recumbent folding and loading. The folding is interpreted to indicate flow of the early-deposited mudstones and we hypothesize that this weak basal layer accommodated the displacement at the base of the faults cutting the younger section, consistent with the interpretation of Nix (1999); Morris and Nix (2000). Dewatering features, such as pipes and flame-structures, indicate that the prodelta sediments were waterlogged at the time of deformation and had not experienced significant compaction.

4.2. Growth section

The growth section is shown in light yellow to orange in Fig. 2. It forms as a series of six offlapping sandstone wedges, labelled SS1–SS6 from youngest to oldest respectively (Fig. 2(D)). These wedges consist of fine- to medium-grained cross-bedded sandstones, 2–9 m thick, with meter-scale truncation and erosion between cross sets. We interpret these facies as migrating subaqeous dunes. The truncation suggests that the dunes formed in shallow distributary channel and distributary-mouth bars in the proximal delta front (channel scours are labelled in Fig. 2(B) and (C)). Cross-sets decrease in thickness from 2 m to a few decimeters away from the faults. This may reflect decreasing flow velocity in a down-current direction as expected in a distributary mouth bar and/or decreased preservation of cross-strata away from the active faults. Decreased preservation of cross strata in the distal hangingwalls suggests that the faults were moving during deposition of the cross-bedded sands. Cross bedding is locally organized into apparently climbing co-sets (e.g. see arrow between sections 9 and 10, Fig. 2), possibly indicating high sand aggradation rates and upstream accretion of bars. Alternatively, cross sets might step landward as rotation on the hangingwall increases towards the fault. The offlapping organization of the growth sands shows that cross-sets step seaward. This suggests that both upstream and downstream accretion of sands has occurred, as is seen in modern river-dominated deltas (Van Heerden & Roberts, 1988). Paleocurrent directions are strongly unimodal and indicate flow to the northwest.

The organization of cross strata suggests that fault movement and sand deposition were roughly synchronous and reflects a complex interplay. This is in distinct contrast to the style of synsedimentary faulting described by Nemec et al. (1988) and by Pulham (1993) in which failure of the delta front and proximal slope occurs first forming a complex seafloor topography that is then later infilled or 'healed' with finer grained prodelta sediments.

Locally sandstones show extensive soft sediment deformation and dewatering structures, such as dish structures and pipes (see sandstone SS4, between sections 9 and 10, Fig. 2). This indicates that growth faulting occurred while sediments were still waterlogged and before significant compaction had occurred.

Much less mudstone was observed in the growth section compared to the pre-growth section, although cross-bedded sandstones can be traced into heterolithic facies in more distal positions. As an example, light yellow SS6 sandstone at the base of measured sections 4 and 5, in Fig. 2(C) correlate with light yellow SS6 heterolithic strata in measured section 10 at the base of the growth section.

4.3. Post-growth section

The overall succession is truncated by a decimeter-thick bed of bioturbated sandstone containing abundant centimeter-diameter *Ophiomorpha* and *Skolithos* burrows (Fig. 2). This bed is in turn overlain by marine shales at the base of the next upward-coarsening succession in Stratigraphic Cycle 2 of Gardner (1995). No mapped faults persist above this bioturbated unit showing that growth faulting ceased with the transgression of the lobe and deposition of this thin sandstone.

5. Structural style

Sets of closely-spaced listric faults separate the mapped section into three major fault blocks, which we label proximal, intermediate, and distal (Fig. 2(D)). Fault Sets A and C are associated with the proximal and distal fault blocks respectively (Fig. 2(D)). A single intermediate Fault B (Fig. 2(D)) separates the intermediate fault block from the proximal fault block. These faults dip to the northwest (seaward) in the same direction that the delta progrades.

Correlative beds traced across faults serve as markers for measuring fault throw and show that the largest throw occurs across Fault Sets A, C and Fault B. A distinct pair of sandstone beds in the pregrowth section at the base of the exposure, for example, coloured yellow and green in Fig. 2(B), is displaced seaward across these faults with a composite throw of nearly 13 m. The greatest throw occurs across Fault Set C (Fig. 2(B) and (D)). The heterolithic pregrowth section curves upward with displacement along the listric faults.

Fault Sets A and C each comprise three faults. Each fault in the set forms landward and upsection of the older fault. Thus in a single fault set, the earliest fault is formed in the most seaward position. With subsequent movement the fault locks and displacement is transferred landward, to the adjacent fault. This has the effect of passively rotating the earlier faults with displacement on the latter. None of the mapped faults extend to the overlying regional flooding surface that caps this delta lobe.

The thick sand intervals of the growth section fill the hangingwalls of the faults. Correlating the sands across the faults in the relatively homogenous growth section is more difficult than in the more heterogeneous pregrowth section because distinctive beds are less obvious. Our correlation relies principally on the stratal geometry, thickness and description.

The prograding sands near the top of the section, (SS1–SS3 in Fig. 2) have a characteristic wedge-shape that is typical of fault growth-stratigraphy. The youngest prograding sand wedge (SS1 in Fig. 2(D)) continues beyond the fault at the northwest limit of the mapped outcrop where it is shown to thicken across the fault. The immediately underlying prograding sand wedge SS2 expands across the two basinward fault segments in Fault-set C. The youngest fault in Fault-set C terminates at the erosional contact separating SS1 and SS2. Similar wedge-shaped geometries can also be seen in SS3 within the proximal fault block and in SS5 in the intermediate fault block. Prograding wedge SS6 also expands across the most basinward fault in Fault-set A, and thins in the intermediate fault block. The thinning of the prograding sand wedges in the deeper sands (SS4–SS6) is less dramatic than in the younger sands and generally they have a thicker flat-stratified form. This fault terminates likewise against the erosional contact between SS3 and SS6.

There is some indication that the distal thinning of sandstones is caused by increased erosion on distal hanging walls. Cross strata in proximal hangingwalls is preserved, such as the thick SS5 sandstones that onlap Fault B.

Bending of the displaced section above the listric faults nucleates conjugate fault sets in the distal ends of the intermediate and distal fault blocks. A pattern of nested conjugate faults with small displacement occurs in a narrow region of the hangingwall of the distal fault block.

In contrast, conjugate faults in the intermediate fault block bound a wide graben bounded by sub-parallel synthetic and antithetic fault pairs. Several small synthetic faults dipping in the same direction as Fault B lie near the center of the intermediate fault block (Fig. 2(B) and (C)). The closely-spaced faults extend over a 5 m wide area, centered on measured section 8 (Fig. 2(B)) and show just centimeters of displacement across individual faults. The longest synthetic faults in the intermediate conjugate fault set terminate at the erosional contact of prograding wedge SS3. An antithetic fault set bounds the wide graben at the northwestern limit of the intermediate fault block. These faults are cut or beheaded by the most landward fault in Fault-set C. Local thickening of the section can be observed in wedge SS5 across these antithetic southeast-dipping faults (Fig. 2).

Closer inspection of the larger faults comprising Fault-sets A, C and Fault B, particularly where they cut the cross-bedded sandstones, shows that they are rarely single through-going features but rather form zones of discrete fault segments spaced a few centimeters apart. These zones may be disaggregation bands (Fisher & Knipe, 1998), narrow zones of rolled and compacted grains, or deformation bands (Aydin, 1978) containing crushed quartz grains. We have not completed a microstructural analysis of the fault zones but hypothesize that grain rolling is a more likely mechanism because the faults are formed early in soft, wet sediment. In places, shale and sand is smeared along fault zones cutting the mud-rich beds in the pre-growth section.

6. Kinematic restoration

Kinematic restoration of the interpreted structure and stratigraphy demonstrates the interplay of the sediment-fill with the fault nucleation and growth and fill history over time (Fig. 3). Kinematic restoration assumes no mechanical properties for the individual layers. An individual bed is restored to its un-faulted state by displacing the section backward, along the fault shape projected to depth, as determined from the hangingwall shape, the mapped fault trace shape and the fault throw (Dula, 1991). From the restoration we calculated the total composite throw and horizontal extension. The bed restoration along the faults is well constrained in the pregrowth section because of the measured fault displacement of marker beds. The restoration is less well constrained across the thick homogeneous sandy growth section because fewer distinctive markers can

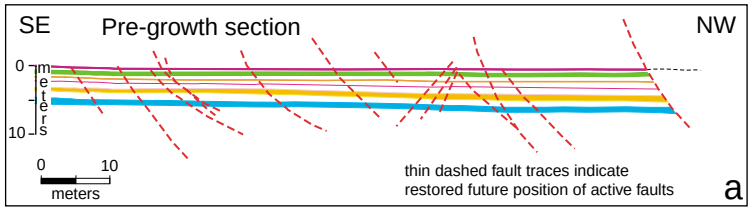
SE
Pre-growth section
NW
0
meters
10
0
10
meters
thin dashed fault traces indicate
restored future position of active faults
a

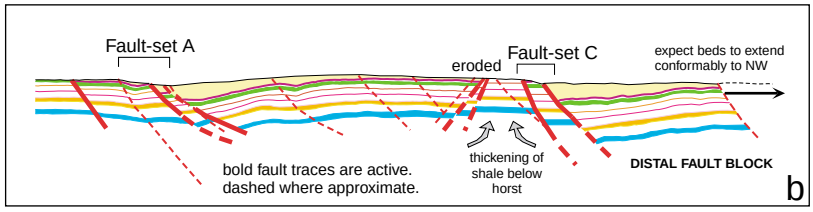
Fault-set A
eroded
Fault-set C
expect beds to extend
conformably to NW
bold fault traces are active.
dashed where approximate.
thickening of
shale below
horst
DISTAL FAULT BLOCK
b

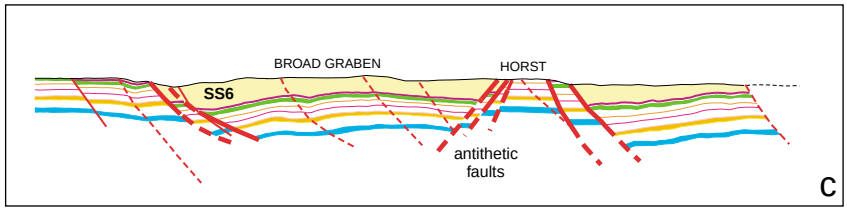
BROAD GRABEN
HORST
SS6
antithetic
faults
c

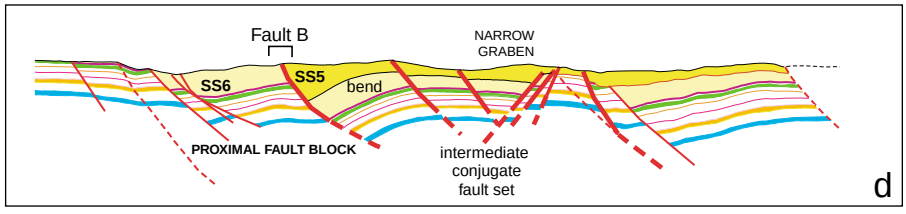
Fault B
NARROW
GRABEN
SS6
SS5
bend
PROXIMAL FAULT BLOCK
intermediate
conjugate
fault set
d

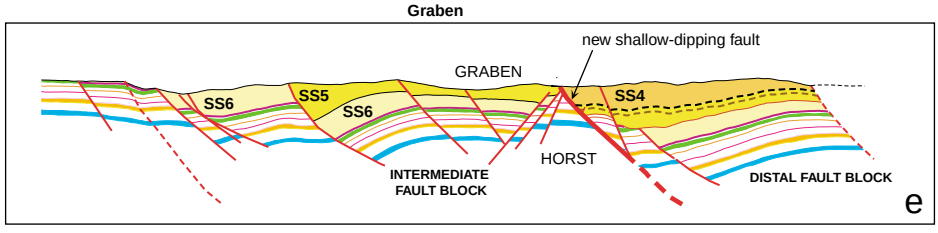
Graben
new shallow-dipping fault
GRABEN
SS6
SS5
SS6
SS4
HORST
INTERMEDIATE
FAULT BLOCK
DISTAL FAULT BLOCK
e

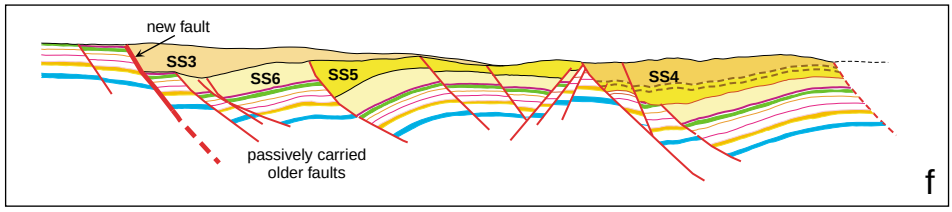
new fault
SS3
SS6
SS5
SS4
passively carried
older faults
f

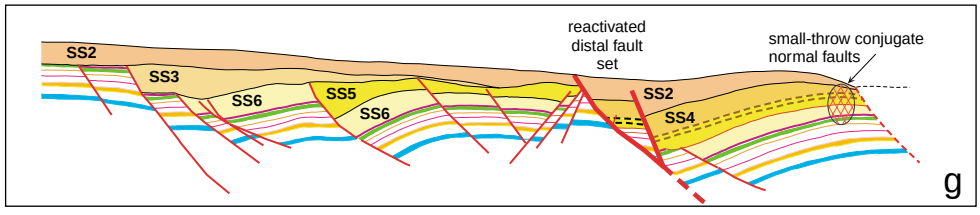
reactivated
distal fault
set
small-throw conjugate
normal faults
SS2
SS3
SS6
SS5
SS6
SS2
SS4
g

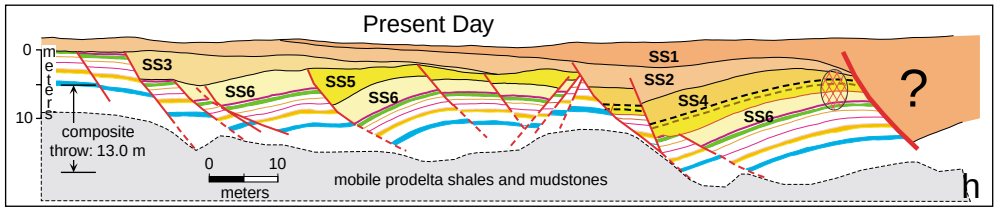
Present Day
0
meters
10
SS3
SS6
SS5
SS6
SS1
SS2
SS4
SS6
?
composite
throw: 13.0 m
0
10
meters
mobile prodelta shales and mudstones
h

be traced across faults in the sands. A residual uneven topography results for each stage of the restoration from the uncertainty in the bed and fault shapes.

The restoration begins with an undeformed pregrowth section (Fig. 3(a)). (Thin dashed red lines represent the future position of faults in the restoration figures.) Fig. 3(b) shows that the proximal and distal fault sets A and C nucleate first with deposition of a thick cross-bedded sand (SS6 yellow layer in Figs. 2 and 3(b)) filling the broad hangingwalls of the faults. (The bold red solid lines in the restorations represent faults active at that stage in the restoration. The red thin lines represent faults that have ceased activity.) Fault-sets A and C initiate as closely-spaced fault pairs, which in map-view may be overlapping terminations or relay ramp (Davies, Crawford, Dula, Cole, & Dorn, 1997) between two en-echelon fault segments.

Antithetic faults develop near the center of the mapped outcrop separating Faul-set A and C (Fig. 2(B) and (C)). Fault-set A and the antithetic faults bound a broad graben and Fault-set C and the antithetic faults bound a narrow horst. Erosion or thinning of weak beds in unconsolidated sands and muds occurs over the horst bounded by the antithetic faults and Faults C (Fig. 3(c)). We hypothesize that mobile shale underlying the section is depleted from the hangingwalls of the faults and thickens into the footwall, filling the space created by the thinning of the overlying section in the horst. Prograding sands of SS6 contemporaneously fill both the broad graben and the hangingwall of Fault-set C. This basal section most likely thins to the northwest beyond the section interpreted.

Fault displacement and deposition of the cross-bedded sands of the SS6 layer into the broad graben bounded by the antithetic faults and Fault-set A bends the section, which initiates Fault B (Fig. 3(d)) separating the proximal and intermediate fault blocks. Numerous small-throw faults also develop in the curved hanging-wall in response to this bending (Fig. 2). This geometry effectively narrows the broader graben, which is now defined by Fault B and the antithetic faults (Fig. 3(d)). Deposition of SS5 fills the hangingwall of Fault B and the hangingwall of the active proximal fault in Fault-set C. The distal fault in set C has ceased movement and is buried with the deposition of SS5.

The development of a new shallow dipping listric fault landward of the previously active faults maintains throw across Fault-set C. This new fault cuts the distal margin of the horst block. Cross-bedded delta front sands (SS4 sandstones in Figs. 2 and 3(e)) fill the space created in the new hanging wall. The older faults in the distal fault set rotate passively to a shallower dip with small displacement.

The delta front sands (SS4 in Fig. 3(e)) are separate from the underlying SS5 sands because they show distinctive soft-sediment sedimentary deformation and are not readily correlated to the other sands. They may be: (1) a unique sand-fill; (2) a correlative unit to the underlying SS5 sand; or (3) a correlative sand to the light orange SS3 prograding sand shown in Fig. 3(f). The data are inconclusive and so we show the deposition as a separate event, but acknowledge that the fault throw may be contemporaneous with the proximal Fault-set A.

Continued seaward progradation of the delta is indicated by the offlapping cross-bedded sandstones of the younger units SS1–SS3. The sand SS3 is deposited first across the most proximal fault in Fault-set A. Bending of the beds due to continued fault displacement nucleates numerous small-throw conjugate fault sets primarily in more thinly bedded facies of the growth section in the distal hanging-wall of Fault-set C. A final prograding succession SS1, fills the unmapped fault block at the NW-edge of the mapped outcrop. These youngest sets of offlapping sands prograde across faults in a systematic seaward sequence.

The restoration shows that no single fault is active throughout the structural history. Faults within the fault sets are active at different times but generally accommodate subsequent activity on a new landward fault in the set. The faults do not show a landward or seaward progression of fault development except in the shallowest prograding sandstone units SS2 and SS1. The total horizontal extension over the mapped outcrop length of 126 m is 33 m.

These observations are consistent with a seismic study of growth faults in the Gulf of Mexico, which showed a polycyclic fault history for several listric growth faults (Cartwright, Bouroullec, James, & Johnson, 1998). Cartwright relates the cyclic growth history of the faults to sediment loading. We assume a similar control for the faults in this study.

7. Discussion

The lack of mudstone clasts or scarp-collapse breccias within the cross-bedded sandstones suggests that topography on the faults was minimal at all times. This supports approximately synchronous deposition of sand with fault movement. As a consequence, it appears that the faults were uniformly initiated with the deposition of the cross bedded sands. An understanding of where deposition of these cross bedded sands occurs in modern delta fronts may give clues as to where and how growth faults nucleate.

Studies of sand deposition in modern shoal-water river-dominated deltas show a highly complex system of bifurcating distributary channels with several orders of channel splitting (Van Heerden & Roberts, 1988). The ‘terminal’ ends of shallow high-order distributary channel

Fig. 3. Sequential kinematic restoration of Ferron growth faults shown in Fig. 2. Faults show no systematic seaward or landward progression but initiate in different places, probably as a consequence of shifting depositional loci of rapidly deposited distributary mouth bar and shallow distributary channel sands. Flow of underlying mobile prodelta mudstones is likely to have accommodated fault movement and overlying sediment-fill.

are 'plugged' by distributary mouth bars. These mouth bars, in turn, cause sand to be deposited immediately upstream. Eventually, frictional deceleration and instability causes the channel to avulse. Depositional loci thus change position at a variety of scales and may shift not only seaward, as the delta progrades, but also landward, as channel plugging causes upstream deposition, and laterally as channels avulse. As demonstrated here, the growth faults initiate in response to deposition of sand in this dynamic proximal delta front area. Because these depositional loci can locally switch and even migrate upstream, associated growth faults show a similar complex pattern of initiation and movement.

These faults are similar to the Namurian deltas described by Rider (1978). Rider suggests that growth faults form as a natural consequence of delta progradation, in which denser sands are deposited over less-dense prodelta muds. Broader-scale growth faults have been interpreted to form in a progressively seaward-stepping fashion, as delta sediments prograde over shelf muds (Bruce, 1983; Evamy et al., 1978). Our data, admittedly over a rather small area, shows that in detail, faults are not initiated or formed in such a progressive fashion.

We suspect that some larger-scale growth faults that are infilled with shallow-water facies may initiate in a manner similar to that interpreted here, as suggested by Rider (1978). However, regional-scale deformation in deltas is invariably tied to settings adjacent to a shelf-slope break, such as in the Gulf of Mexico (e.g. Winker, 1982) or Niger delta (Evamy et al., 1978). Large-scale faulting is enhanced by gravity-driven slumping and sliding on the continental slope, and the presence of thick underlying overpressured muds or salt (e.g. Martinsen, 1989; Pulham, 1993; Winker, 1982; Winker & Edwards, 1983). Thinner underlying mobile muds and smaller slopes, such as occur in intracratonic settings or farther inboard on the continental shelf, allow less accommodation for growth faulted structures (c.f. Brown, Cleaves, & Erxleben, 1973; Tye et al, 1999).

In this study, larger-scale synsedimentary structures were unable to form because deposition occurred into a large shallow embayment of the Cretaceous seaway formed within an intracractonic foreland basin with no shelf-slope break. Tectonic tilting likely formed this embayment. The active tectonic setting also likely caused earthquakes that may have been responsible for liquefying the prodelta mudstones of the Tununk, helping to initiate some of the faulting.

These faults are also different from faults that form on a slope, such the Cretaceous faults in Spitzbergen, documented by Nemec et al. (1988) and Pulham (1993). Slumps naturally form on slopes, because of downslope gravitational instability, which is enhanced where slope sediments are rapidly deposited and easily liquefied. Slumping occurs along faults and forms a complex sea-floor topography. Deltas subsequently build over these areas and the faulted topography is filled with deep-water delta front turbidites and prodelta mudstones, vs. the shallow-water facies documented here. If movement continues on faults initiated on a slope, younger stages of fill may comprise shallow water facies, but there will be an earlier deeper-water fill stage.

It appears that growth faults can form in wide variety of tectonic settings and are not limited to continental margins or shelf edge deltas, although the scale of faulting may be highly dependent on basin type, tectonic setting, and thickness and type of underlying sediment.

8. Implications for exploration and production

These growth-faults show offset of a few meters, which is well below the scale of features typically imaged by conventional 2D or 3D seismic data. Fault and fracture patterns often have a similar expression at a range of scales suggesting a self-similar geometry (Tchalenko, 1970). We suspect that small-scale growth faulting is common, even in regional-scale growth faults in areas such as the Niger delta or in the Gulf Coast of the USA, but may not be well imaged. Growth-faulted strata at a scale similar to that mapped in this study have been described with limited data in other fluvial-deltaic reservoirs such as the supergiant Prudhoe Bay field in Alaska (Tye et al., 1999). In these types of fields, the interpretation of complex 3D geometry is incomplete. Use of these outcrop analogs should be considered in placement of horizontal production wells and to explain anomalous production. Local over-thickening of sandstones may provide additional reserves which may be missed in reservoirs delineated on the basis of conventional seismic surveys or widely-spaced well logs. Evidence for small-scale synsedimentary growth faulting may be found in dip-meter logs, borehole imaging logs, or in cores which can be compared to the facies and dip-changes documented in this outcrop study.

9. Conclusions

1. Growth faults initiated with deposition of dense, cross bedded sandstones deposited in proximal distributary mouth bars, over less-dense, mobile prodelta mudstones. Changes in the position of active faults through time reflect shifting depositional loci within the dynamic proximal delta front environment.
2. Within the admittedly small area studied, we see no systematic seaward or landward progression of fault development except in the youngest prograding sands. Locally, faults within closely-spaced fault sets step landward as they cut younger section.
3. Although fault blocks are reactivated, individual faults are rarely reactivated. Instead, new faults are formed during subsequent filling of the fault blocks. A single, through-going, long-lived fault was not mapped within any given fault block. Rather, complex sets of faults are active at different times.

4. Growth faulting is accommodated by deformation and movement associated with underlying mobile shales.
5. The systematic decrease in cross-stratal thicknesses away from a given fault likely reflects decreasing preservation in distal hangingwalls but may also be due to a downstream decrease in flow velocity. The growth strata represent the best potential reservoir quality and may have significance for reservoir prediction in subsurface settings.

Acknowledgements

Financial support was kindly provided by ARCO. Figures were drafted by L. Bradshaw. Reviews by Tony Reynolds and an anonymous reviewer significantly improved the manuscript.

References

Aydin, A. (1978). Small faults as deformation bands in sandstone. *Pure and Applied Geophysics*, *116*, 931–942.

Bhattacharya, J. P., & Walker, R. G. (1992). Deltas. In R. G. Walker, & N. P. James, *Facies models: response to sea-level change* (pp. 157–177). Geological Association of Canada.

Bishop, D. J., Buchanan, P. G., & Bishop, C. J. (1995). Gravity-driven, thin-skinned extension above Zechstein Group evaporites in the western central North Sea: an application of computer-aided section restoration techniques. *Marine and Petroleum Geology*, *12*, 115–135.

Brown, L. F. Jr., Cleaves, A. W., II, & Erxleben, A. W. (1973). Pennsylvanian depositional systems in North-Central Texas: A guide for interpreting terrigenous clastic facies in a cratonic basin. Guidebook No. 14, Bureau of Economic Geology, University of Texas at Austin.

Bruce, C. (1983). Shale tectonics, Texas coastal area growth faults. In A. W. Bally (Ed.), *Seismic expression of structural styles*. American Association of Petroleum Geologists Studies in Geology 15, pp. 2.3.1–2.3.6.

Busch, D. A. (1975). Influence of growth faulting on sedimentation and prospect evaluation. *American Association of Petroleum Geologists Bulletin*, *59*, 217–230.

Cartwright, J., Bouroullec, R., James, D., & Johnson, H. (1998). Polycyclic motion history of some Gulf Coast growth faults from high-resolution displacement analysis. *Geology*, *26* (9), 819–822.

Davies, R. K., Crawford, M., Dula Jr., W. F., Cole, M. J., & Dorn, G. A. (1997). Outcrop interpretation of seismic-scale normal faults in southern Oregon: description of structural styles and evaluation of subsurface interpretation methods. *The Leading Edge*, *16* (8), 1135–1141.

Diegel, F. A., Karlo, J. F., Schuster, D. C., Shoup, R. C., & Tauvers, P. R.(1995). Cenozoic structural evolution and tectono-stratigraphic framework of the northern gulf coast continental margin. In M. P. A. Jackson, D. G. Roberts, S. Snelson (Eds.), *Salt tectonics: a global perspective*. American Association of Petroleum Geologists Memoir 65, 109–151.

Dula Jr, W. F. (1991). Geometric models of listric normal faults and rollover folds. *American Association of Petroleum Geologists Bulletin*, *75*, 1609–1625.

Edwards, M. B. (1976). Growth faults in upper Triassic deltaic sediments, Svalbard. *American Association of Petroleum Geologists Bulletin*, *60*, 341–355.

Elliot, T., & Lapido, K. O. (1981). Syn-sedimentary gravity slides (growth faults) in the Coal Measures of South Wales. *Nature*, *291*, 220–291.

Evamy, D. D., Haremboure, J., Kamerling, P., Knapp, W. A., Molloy, F. A., & Rowlands, P. H. (1978). Hydrocarbon habitat of Tertiary Niger delta. *American Association of Petroleum Geologists Bulletin*, *62*, 1–39.

Fisher, Q. J., & Knipe, R. J. (1998). Fault sealing processes in siliciclastic sediments. In G. Jones, Q. J. Fisher, R.J. Knipe (Eds.), *Faulting, fault sealing and fluid flow in hydrocarbon reservoirs*. Geological Society, London, Special Publications 147, 117–134.

Galloway, W. E., Hobday, D. K., & Magara, K. (1982). Frio formation of Texas Gulf coastal plain-depositional systems, structural framework and hydrocarbon distribution. *American Association of Petroleum Geologists Bulletin*, *66*, 649–688.

Gardner, M. (1995). Tectonic and eustatic controls on the stratal architecture of mid-Cretaceous stratigraphic sequences, central western interior foreland basin of North America. In S. L. Dorobek, G. M. Ross (Eds.), *Stratigraphic evolution of foreland basins*. SEPM Special Publication 52, 243–281.

Gingras, M. K., MacEachern, J. A., & Pemberton, S. G. (1998). A comparative analysis of the ichnology of wave- and river-dominated allomembers of the Upper Cretaceous Dunvegan Formation. *Bulletin of Canadian Petroleum Geology*, *46*, 51–73.

Martinsen, O. J. (1989). Styles of soft-sediment deformation on a Namurian (Carboniferous) delta slope, Western Irish Namurian basin, Ireland. In M. K. G. Whateley, K. T. Pickering (Eds.), *Deltas: sites and traps for fossil fuels*. Oxford: Blackwell Scientific Publications, Geological Society Special Publication 41, 167–177.

Morris, T. H., & Nix, T. L. (2000). Structural and sedimentologic elements of an evolving growth fault system: outcrop and photomosaic analysis of the Ferron Sandstone, Utah. *American Association of Petroleum Geologists Annual Meeting Abstract*, 84.

Moslow, T. F., & Pemberton, S. G. (1988). An integrated approach to the sedimentological analysis of some lower Cretaceous shoreface and delta front sandstone sequences. In D. P. James, D. A. Leckie (Eds.), *Sequences, stratigraphy, sedimentology; surface and subsurface*. Canadian Society of Petroleum Geologists, Memoir 15, 373–386.

Nemec, W., Steel, R. J., Gjelberg, J., Collinson, J. D., Prestholm, E., & Oxnevad, I. E. (1988). Anatomy of a collapsed and re-established delta front in Lower Cretaceous of Eastern Spitsbergen: gravitational sliding and sedimentation processes. *American Association of Petroleum Geologists, Bulletin*, *72*, 454–476.

Nix, T. L. (1999). *Detailed outcrop analysis of a growth fault system and associated structural and sedimentological elements, Ferron sandstone, Utah*. Unpublished MS thesis, Brigham Young University.

Pulham, A. J. (1993). Variations on slope deposition, Pliocene-Pleistocene, offshore Louisiana, Northeast Gulf of Mexico. In P. Weimer, H. W. Posamantier (Eds.), *Siliciclastic sequence stratigraphy, recent developments and applications*. American Association of Petroleum Geologists Memoir 58, 199–233.

Rider, M. H. (1978). Growth faults in Carboniferous of Western Ireland. *American Association of Petroleum Geologists Bulletin*, *62*, 2191–2213.

Ryer, T. A. (1984). Transgressive-regressive cycles and the occurrence of coal in some Upper Cretaceous strata of Utah, USA. *IAS Special Publication*, *7*, 217–227.

Ryer, T. A., & McPhillips, M. (1983). Early Late Cretaceous paleogeography of East-Central Utah. In M. W. Reynolds, E. D. Dolly (Eds.), *Mesozoic paleogeography of west-central United States*. Rocky Mountain Section, SEPM, Symposium 2, 253–271.

Tchalenko, J. S. (1970). Similarities between shear zones of different magnitudes. *Bull. Geol. Soc. Am.*, *81*, 1625–1640.

Tye, R. S., Bhattacharya, J. P., Lorsong, J. A., Sindelar, S. T., Knock, D. G., Puls, D. D., & Levinson, R. A. (1999). Geology and stratigraphy of fluvio-deltaic deposits in the Ivishak Formation: applications for development of Prudhoe Bay Field, Alaska. *American Association of Petroleum Geologists, Bulletin*, *83*, 1588–1623.

Van Heerden, I. L., & Roberts, H. H. (1988). Facies development of

Atchafalaya delta, Louisiana: a modern bayhead delta. *American Association of Petroleum Geologists, Bulletin*, *72*, 439–453.

Winker, C. D. (1982). Cenozoic shelf margins, northwestern Gulf of Mexico. *Transactions—Gulf Coast Association of Geological Societies*, *32*, 427–448.

Winker, C. D., & Edwards, M. B. (1983). Unstable progradational clastic shelf margins. In D. J. Stanley, G. T. Moore (Eds.), *The shelfbreak: critical interface on continental margins*. SEPM Special Publication, Tulsa, Oklahoma 33, 139–157.